Published in final edited form as:
Eur J Immunol. 2010 September ; 40(9): 2618–2631. doi:10.1002/eji.200940134.

Glycosylation contributes to variability in expression of MCMV m157 and enhances stability of interaction with the NK cell receptor, Ly49H

Natalya V. Guseva[1], **Colleen A. Fullenkamp**[1], **Paul W. Naumann**[1], **Michael R. Shey**[2], **Zuhair K. Ballas**[2,3], **Jon C.D. Houtman**[4], **Catherine A. Forbes**[5,6], **Anthony A. Scalzo**[5,6], and **Jonathan W. Heusel**[1]

[1]Department of Pathology, Roy J. and Lucille A. Carver College of Medicine, Iowa City, Iowa 52242

[2]Iowa City VA Medical Center, Roy J. and Lucille A. Carver College of Medicine, Iowa City, Iowa 52242

[3]Department of Internal Medicine, Roy J. and Lucille A. Carver College of Medicine, Iowa City, Iowa 52242

[4]Department of Microbiology, Roy J. and Lucille A. Carver College of Medicine, Iowa City, Iowa 52242

[5]Centre for Ophthalmology and Vision Science, M517, University of Western Australia, 35 Stirling Hwy, Crawley, WA 6009, Australia

[6]Centre for Experimental Immunology, Lions Eye Institute, 2 Verdun St, Nedlands, WA 6009, Australia

Summary

Natural killer (NK) cell-mediated resistance to murine cytomegalovirus (MCMV) is controlled by allelic Ly49 receptors, including activating Ly49H (C57BL/6 strain) and inhibitory Ly49I (129 strain), which specifically recognize MCMV m157, a glycosylphosphatidylinositol-linked protein with homology to MHC class I. Although the Ly49 receptors retain significant homology to classic carbohydrate-binding lectins, the role of glycosylation in ligand binding is unclear. Herein we show that m157 is expressed in multiple, differentially N-glycosylated isoforms in m157-transduced or MCMV-infected cells. We used site-directed mutagenesis to express single and combinatorial asparagine (N)-to-glutamine (Q) mutations at N178, N187, N213, and N267 in myeloid and fibroblast cell lines. Progressive loss of N-linked glycans leads to a significant reduction of total cellular m157 abundance, although all variably glycosylated m157 isoforms are expressed at the cell surface and retain the capacity to activate Ly49H^{B6} and Ly49I^{129} reporter cells and Ly49H^{+} NK cells. However, the complete lack of N-linked glycans on m157 destabilized the m157-Ly49H interaction and prevented physical transfer of m157 to Ly49H-expressing cells. Thus, glycosylation on m157 enhances expression and binding to Ly49H, factors that may impact the interaction between NK cells and MCMV *in vivo* where receptor-ligand interactions are more limiting.

Address correspondence to: Jonathan W. Heusel, MD, PhD, 1030 Medical Laboratories, 200 Hawkins Drive, Iowa City, IA 52242, Tel: (319) 335-8217/Fax: (319) 335-8453, jon-heusel@uiowa.edu.

Conflict of interest
Authors have no financial conflicts of interest.

Keywords

NK cell; glycosylation; lectin; viral immunity

Introduction

Natural killer (NK) cells are vital components of the integrated immune response to a wide variety of pathogens; their responses during herpesvirus infections are particularly well characterized [1–4]. The activation of individual NK cells depend upon the integration of stimulatory and inhibitory signals mediated through multiple receptor systems, including members of the C-type lectin receptor (CLR) superfamily. The CLRs are defined by the presence of a highly conserved extracellular carbohydrate recognition domain (CRD) found in over 1,000 diverse proteins, including the prototypical mannose binding receptor (MBP-A) [5]. The group V CLRs include NKR-P1, CD94, and NKG2 receptors that are conserved in rodents and primates, and the Ly49 receptors in rodents. The loci encoding the group V CLR are organized as conserved gene clusters in syntenic regions of mouse chromosome 6 and human chromosome 12. Each CLR gene cluster encodes activating receptors such as Ly49H and NKG2D that mediate potent antimicrobial and antitumor responses, as well as inhibitory receptors such as Ly49A, C, and I and CD94/NKG2A that bind that bind constitutively expressed cell surface ‘self’ ligands providing for tonic inhibition in a healthy (non-stressed) environment (reviewed in ref. [6,7]).

As regulators of potent lymphocyte effector functions, it is not surprising that the group V CLRs are targets for immune evasion mechanisms such as those described for cytomegalovirus infections in humans and rodents involving NKG2D, CD94/NKG2A, NKR-P1B, and inhibitory Ly49 receptors [1,8–13]. Among these, MCMV m157 is unique in that it is also a specific ligand for an activating receptor in the Ly49 family, Ly49H [8,14]. The presence of Ly49H in the C57BL/6 (B6) strain confers a dominant resistance mechanism for control of acute MCMV infection known as *Cmv-1* [15–18]. Given that m157 may interact with additional inhibitory Ly49 receptors [9] and that the activating Ly49 receptor genes likely evolved after their highly homologous inhibitory ‘clustermates’ [19], it would appear that *ly49h* represents a dynamic murine host response to selective pressure exerted by MCMV [1,20,21]. As such, the interaction between m157 and its cognate Ly49 receptors represents an opportunity to understand the molecular parameters governing both NK cell tolerance and activation.

Unlike the true calcium-dependent (C-type) lectins, the group V CLRs do not require calcium for binding of their ligands, which are primarily MHC class I and related cell surface glycoproteins [7,11,22,23]. Furthermore, cognate interactions involving Ly49 (and NKG2D) receptors result in a significant degree of physcial ligand transfer (trogocytosis) [24–28], which may occur for many, if not all, of the receptors in this class. However, the role for carbohydrates in determining ligand specificity or other aspects of lectin-like receptor function is not clear. To investigate the contribution of potential N-linked glycosylation toward m157 heterogeneity and recognition by Ly49 receptors, we undertook site-directed mutagenesis of four N-linked glycosylation sites in m157 (N178, N187, N213 and N267) and expressed single and combinatorial N-glycosylation mutants of m157 in cell lines representing myeloid and fibroblast lineages. These m157-transduced cell lines were used to evaluate the role of N-linked glycosylation of m157 in its functional and physical interactions with cognate Ly49 receptors expressed on reporter cells and NK cells.

Results

Differential expression of MCMV m157 isoforms among m157-transduced cells

We previously observed expression of multiple m157 isoforms in MCMV-infected fibroblasts, macrophages, and dendritic cells that differed in both abundance and relative molecular mass [29]. To better characterize m157 expression in different cell types, we transduced C1498 myeloid leukemia cells, P815 mastocytoma cells, and the two fibroblast lines NIH-3T3 and BALB-3T12 with *wt*-m157 using retroviral transduction. As shown in Fig. 1A, each of these cell types is able to support robust cell surface expression of m157 as assessed by flow cytometry. Western blot analysis of cell lysates revealed multiple m157 isoforms expressed in all transduced lines ranging from ~42–55 kDa (Fig. 1B), sizes in excess of the predicted Mw of ~32 kDa for the putative mature m157 polypeptide (residues Ile22-Arg306 [30]). As was observed for MCMV-infected cells [29], expression of m157 isoforms differs in abundance and apparent mass between the transduced cell types. Together with our previous findings [29], these data suggest that m157 undergoes posttranslational modification that is differentially regulated among transduced (or MCMV-infected) cell types.

MCMV m157 isoforms are differentially N-glycosylated

The m157 open reading frame encodes a 329 amino acid polypeptide that is predicted to undergo amino terminal processing of 21 amino acids (signal peptide) and cleavage of the last 22 residues at the carboxyl terminus in conjunction with the addition of a GPI membrane linkage [8,14,29,31]. Within the mature m157 polypeptide of 286 residues are four putative sites for asparagine-linked glycosylation (NxT/S): N178, N187, N213, and N267 (a fifth site at N284 is not considered since it coincides with the predicted omega (ω)-site for GPI modification at Ser286) (Fig. 2A). To directly evaluate whether m157 is glycosylated, lysates from m157-transduced cells were incubated with endoglycosidase H (Endo H), which removes only high mannose and some hybrid types of N-linked carbohydrates (resistance to Endo H indicates glycosylation has progressed beyond the cis-Golgi), or with peptide N-glycosidase F (PNGase F) which removes all types of N-linked glycans. As shown in Fig. 2B, Endo H treatment of m157-transduced cells resulted in a new band of 32 kDa being detected in low abundance for C1498 and P815 cells (Fig. 2B, lanes 2 and 5) and higher abundance in the 3T3 and 3T12 fibroblasts (lanes 8 and 11). This suggests that in fibroblasts more m157 accumulates in the ER and/or cis-Golgi during glycosylation as compared to the myeloid cell lines. Endo H treatment did not alter significantly the higher *Mw* m157 isoforms; however, treatment with PNGase F resulted in a similar reduction of all m157 isoforms to a single band at ~32 kDa for all m157-expressing cell lines.

In MCMV infected cells, m157 is also differentially N-glycosylated. Fibroblasts express at least three m157 isoforms (42–50 kDa), while IC-21 macrophages and DC2.4 dendritic cells express isoforms of similar size at 42 and 48 kDa plus a larger species at >50 kDa, but lack the predominant species at ~45 kDa seen in fibroblasts (Fig. 2C). Treatment of virally infected cells with Endo H led to visible disappearance of the low Mw band (42kDa) suggesting this band represents m157 modified only by high mannose. As was observed for m157-transduced cells, all m157 isoforms are reduced to ~32 kDa following PNGase F treatment of the MCMV-infected cell lysates. These results indicate that despite differential N-glycosylation patterns among transduced and MCMV-infected cells, m157 protein is otherwise similarly posttranslationally processed. The observed mass of fully deglycosylated m157 species in all cells (a single species of ~32 kDa) is consistent with utilization of the ω-site at Ser286 for GPI addition, and a mature m157 polypeptide of 286 residues.

Site-directed mutagenesis of m157 reveals utilization of four N-glycosylation sites—the progressive loss of N-linked glycans results in reduced abundance of total cellular m157

To determine which of four putative N-glycosylation sites in the mature m157 protein are modified, we undertook PCR-mediated site-directed mutagenesis at positions N178, N187, N213, and N267, converting each asparagine to glutamine (N→Q). In addition, we generated a double glutamine substitution mutant at positions N178 and N187 (N178,187Q), a triple mutant at the additional N213 position (N178,187,213Q), and the quadruple mutant (N178,187,213,267Q). Using retroviral transduction, each of these m157 mutant cDNA cassettes was introduced into C1498, P815 and 3T12 cells. Flow cytometry of each transduced cell line revealed that each of the seven m157 N-glycosylation site variants shows surface m157 expression, although the triple- and quadruple-mutants have reduced mean fluorescence intensity (MFI), indicating a lower m157 density (Fig. 3A). We noted a similar expression pattern for the seven m157 N-glycosylation mutants in transduced P815 and 3T12 cells (data not shown). The reduced level of cell surface unglycosyalted m157 in m157-N178,187,213,267Q-transduced cells is not due to intracellular retention, and does not result in altered subcellular distribution of m157 as assessed by confocal microscopy; indeed, very little intracellular staining is observed for either *wt*- or unglycosylated m157, including the Golgi (as determined by colocalization with giantin [32]; data not shown).

In order to verify the glycosylation status of each mutant, cell lysates were treated with PNGase F and analyzed by western blotting. As shown in Fig. 3B, there was a demonstrable decrease in m157 mass for untreated lysates prepared from each of the four single N-glycosylation mutants (N178Q, N187Q, N213Q, and N267Q) compared to *wt*-m157. The double and triple mutants (N178, 187Q and N178,187,213Q) showed even greater reduction in size, reflecting the cumulative loss of N-linked glycans. The quadruple mutant showed no difference in mass compared to the fully deglycosylated *wt*-m157 following PNGase F treatment, indicating that N-linked glycosylation is responsible for the observed differences in molecular mass for all m157 isoforms expressed in the m157-transduced lines. Among the four single N-glycosylation site mutants, m157 protein was readily detectable; however, the abundance of m157 in lysates from the double, triple and quadruple mutants was dramatically reduced. As expected, the reduced abundance of m157 protein was not due to transcriptional differences among the m157-transduced cell lines, as determined by RT-PCR using primers specific for m157 and GAPDH mRNA (data not shown). In addition, the reduced total cellular abundance of unglycosylated m157 is not due to accelerated proteasomal or lysosomal degradation, or altered ubiquitination (Suppl Fig. 1). However, treatment of the *wt*-and N178,187,213,267Q mutant-m157-expressing cell lines with cyclohexamide revealed that the unglycosylated m157 has a shorter half-life compared to the *wt*-m157 (23% vs. 99% remaining after 24 hr, respectively; Suppl Fig. 2).

We also verified that all the variably glycosylated m157 mutants remain GPI-linked by treatment of C1498 cells expressing *wt*- or mutant m157 variants with phosphatidylinositol-specific phospholipase C (PI-PLC). As shown in Fig. 3C for *wt*-m157 and all N-glycosylation mutants, soluble m157 was detected in supernatants after PI-PLC treatment. These data also indicate that the reduction in apparent m157 abundance observed for the double, triple, and quadruple N-glycosylation site mutants is most likely not due to secretion or shedding, since no significant m157 is detected in the supernatants of untreated samples for these mutant m157-expressing cell lines.

N-linked glycosylation of m157 is dispensable for activation of Ly49H and Ly49I^{129} reporter cells, as well as Ly49H^{+} NK cells, in vitro

To assess functional consequences of individual and multiple N-glycosylation site mutations in m157, we compared the capacity of each of the seven m157 mutants with *wt*-m157 to

activate Ly49H-expressing HD12 reporter cells (quantitatively measured by conversion of the colorimetric substrate chlorphenol red β-D-galactopyranoside, CPRG) [14]. As shown in Fig. 4A, all of the N-glycosylation mutants retained significant Ly49H- activating capacity during the 16–20 hr coincubation; only the fully unglycosylated N178,187,213,267Q mutant showed a moderate reduction in β-galactosidase activity. Similar results were observed for both P815 and 3T12 cells transduced with *wt*-m157 or each of the seven N-glycosylation mutants (data not shown). The specificity of Ly49H activation by each mutant was verified by pre-incubation with anti-m157 mAb 6D5, which completely blocks activation of the HD12 reporters ([29] and data not shown). However, addition of anti-Ly49H mAb 3D10 (1 or 10 μg/mL) at the beginning of coincubation led to complete blockade of HD12 reporter activity when stimulated by fully unglycosylated m157-N178,187,213,267Q, compared to ~50% reduction of activity when stimulated by *wt*-m157 (Fig.4A, right panel). This interesting result suggests that although anti-Ly49H mAb 3D10 is able to bind Ly49H in complex with m157 (as is evident from our previous [29] and current 3D10 immunoprecipitations), this binding is more competitive for unglycosylated m157, perhaps reflecting a lower stability of the Ly49H-unglycosylated m157 complex.

We also tested whether the panel of C1498 cells expressing m157 N-glycosylation mutants could activate reporter cells expressing Ly49I from the 129 strain. Since Ly49I is an inhibitory receptor, the extracellular domain Ly49I was fused in-frame to the transmembrane domain of Ly49H to generate a chimeric Ly49HI^{129} receptor capable of activating the *lacZ* reporter (HI-129 cells). As a control, BWZ.36 reporters expressing a chimeric Ly49I receptor from C57BL/6 mice (HI-B6 cells) were also tested (the allelic Ly49I^{B6} does not bind m157 [8]). As for HD12 cells, all N-glycosylation mutants of m157 retained the capacity to activate Ly49HI^{129} reporters, and this activation was blocked specifically by mAb 6D5. As expected, neither *wt*-m157 nor any of the N-glycosylation mutants activated Ly49HI^{B6} reporters (Suppl. Fig. 3). Thus, both Ly49H and Ly49I^{129} receptors are able to recognize variably N-glycosylated isoforms of m157 expressed on transduced cells.

Next, we tested freshly prepared splenic NK cells from RAG1$^{-/-}$ mice (B6 genetic background) for activation in response to stimulation by transduced cells expressing *wt*-m157 or each of the seven N-glycosylation mutants as measured by intracellular IFN-γ and MIP-1α production, which are secreted in parallel by activated NK cells [33]. Ly49H is expressed on ~50% of NK cells in the C57BL/6 strain [34], and the Ly49H$^+$ NK cell subset is specifically activated during MCMV infection [35] and by transduced cells expressing m157 [8,10,14,29]. NK cell production of MIP-1α in response to stimulation by *wt*-m157 and each of the N-glycosylation variants is shown in Fig. 4B; similar results were obtained for NK cell IFN-γ production stimulated by all seven glycosylation mutants (Fig. 4C and data not shown). It is clear that lack of N-linked glycans at any and all positions for m157 expressed by transduced cells has no significant effect on the capacity to activate Ly49H$^+$ NK cells. Note that cytokine production is confined to the Ly49H$^+$ NK cell subset (detected by mAb 3D10), which typically shows marked downregulation of cell surface Ly49H at the relatively high effector:stimulator ratio of 1:1 used in these assays [14]. Interestingly, among the cytokine-producing NK cells, we observed consistently reduced Ly49H downregulation on NK cells following interactions with transduced cells expressing unglycosylated m157 (e.g., Fig. 4C). This may reflect fewer Ly49H interactions with unglycosylated m157 (due to the lower surface density of m157 on C1498-m157-N178,187,213,267Q cells) and/or a lower stability of the receptor-ligand complexes. Since MCMV-infected cells also promote robust Ly49H downregulation [14], yet express very low levels of m157 ([31] and data not shown), a qualitative effect provided by m157 glycosylation cannot be ruled out.

We also tested the capacity of unglycosylated m157 to activate NK cell cytotoxicity. As shown in Fig. 4D, the C1498-m157-N178,187,213,267Q targets were lysed nearly as effectively as C1498-m157wt targets, and this killing was specifically blocked by anti-m157 mAb 6D5. As we observed for the HD12 reporters, Ly49H-mediated killing of the unglycosylated m157-expressing targets was slightly lower compared to C1498-m157wt targets, most likely reflecting the difference in surface density of m157 (e.g., Fig. 3A). Curiously, this difference was not evident for cytokine secretion by $Ly49H^+$ NK cells (Fig. 4C). These data indicate that although Ly49H-mediated activation of cytokine production and cytotoxicity are not prevented by a partial or complete lack of N-glycosylation on m157 expressed at high level on transduced cells, the complete lack of glycosylation may qualitatively affect the Ly49H-m157 interaction, as measured by Ly49H receptor downregulation.

Lack of N-linked glycosylation decreases the stability of Ly49H-m157 interactions measured by coimmunoprecipitation or live cell conjugate dissociation

The increased sensitivity of HD12 reporters to mAb 3D10-mediated blockade during interaction with fully unglycosylated m157 (Fig. 4A), and the reduced capacity of this quadruple mutant to mediate Ly49H receptor downregulation on NK cells (Fig. 4B, C) prompted us to investigate the stability of interaction between Ly49H and unglycosylted m157. Previously, we demonstrated a reduced Ly49H-binding capacity for m157 variants harboring nonconservative mutations at positions Ile153 and Lys161, as assessed by immunoprecipitation following coincubation of C1498 cells expressing these m157 variants together with HD12 cells [29]. First we verified that 3D10 could specifically coimmunoprecipitate *wt*-m157 and fully unglycosylated m157 (quadruple N178,187,213,267Q mutant) following 10 min of coincubation and that the vast majority of m157 coimmunoprecipitated by 3D10 requires interaction of intact cells (minimal m157-Ly49H interaction in a simple mixture of lysates, Suppl. Fig. 4). This result is in agreement with our observation that anti-Ly49H mAb 3D10 does not completely disrupt the Ly49H-m157 interaction ([29] and Fig. 4A). Next, mixtures of HD12 cells and C1498 cells expressing *wt*-m157 or each of the seven N-glycosylation mutants were incubated for 10 or 40 min (37 °C/5% CO_2) prior to Ly49H immunoprecipitation (mAb 3D10). Coimmunoprecipitated m157 was detected by anti-m157 mAb 6H121 in the subsequent western blot. As shown in Fig. 5A, *wt*-m157 and all of the N-glycosylation mutants bind to Ly49H after 10 min of coincubation; however, following 40 min of coincubation there is marked reduction of coimmunoprecipitated unglycosylated m157 (N178,187,213,267Q mutant), consistent with a significant reduction of binding to Ly49H at this time point. Loading controls for β-actin and the relative abundance of m157 in each sample before Ly49H immunoprecipitation are shown (bottom panel, lysate input), indicating that 3D10-mediated coimmunoprecipitation concentrates m157 at the cell surface relative to the total lysate (as expected), and that the loss of fully unglycosylated m157 after 40 min is not due simply to a reduced overall abundance, since the double- and triple-mutant m157 isoforms are clearly detected despite a similarly reduced overall abundance (see also Fig. 3B).

Since cell surface expression of unglycosylated m157 was consistently lower than for *wt*-m157 across all cell lines, we generated soluble m157-Fc fusion proteins to more quantitatively measure differences in stability of Ly49H-m157 binding attributable to glycosylation. DNA cassettes encoding the extracellular domain of *wt*-m157 [8], or the quadruple N178,187,213,267Q mutant, fused in-frame to human immunoglobulin Fc were transfected into COS-7 cells. Culture supernatants were collected and tested directly, or purified over protein-G mini-columns. Although the purity of these reagents was comparably high, we found that COS-7 cell production of soluble unglycosylated m157-Fc proteins was lower than that of *wt*-m157-Fc (Suppl. Fig. 5), as was observed for m157

expression in C1498 cells. When an equal mass of each purified m157-Fc protein was fluorescently labeled and then used to stain HD12 cells, we found that the unglycosylated m157-Fc showed considerably lower binding to HD12 cells at equilibrium (Suppl. Fig. 6). Since the total amount of unglycosylated m157-Fc was limiting, we tested the strength of Ly49H binding by measuring the decay of fluorescent-m157-Fc staining of HD12 cells in the presence of cold competitors to Ly49H (mAb 3D10) or m157 (mAb 6D5) binding. The amounts of *wt*- and unglycosylated m157-Fc supernatants were adjusted to produce equivalent staining of HD12 cells (Fig. 5B). We then added an excess of either 3D10 or 6D5 and measured the decrease in fluorescence over the following 40 min. As shown in Fig. 5C, the loss of fluorescence from HD12 cells stained with unglycosylated m157-Fc was more rapid and greater in magnitude, regardless of whether we were blocking the ligand or the receptor. Similar results were obtained when we measured the dissociation of viable cellular conjugates formed between PKH26-labeled HD12 cells and CFSE-labeled C1498 cells expressing either *wt*-m157 or the unglycosylated N178,187,213,267Q mutant over the same time period (data not shown). These results show that N-linked glycans on m157 stabilize binding to Ly49H at the cell surface, and suggest that the enhanced stability afforded by glycosylation contributes to the strength of cell-cell contacts.

Glycosylation of m157 facilitates transient physical interaction with Ly49H

The inability to coimmunoprecipitate m157-N178,187,213,267Q with Ly49H at 40 min of coincubation was similar to what we previously observed for m157-I153T, -K161N, -D109N and -R158Q variants [29]. In order to verify that both receptor and ligand were available for interaction at time points longer than 10 min, we assessed the cell mixtures by flow cytometry for surface expression of m157 and Ly49H at times ranging from 5 to 185 min of coincubation (earliest 5 min time point reflects processing for surface marker staining immediately after mixing the cells). In addition to expression of Ly49H, we established the identity of HD12 cells by CFSE-labeling prior to coincubation. The results for HD12 coincubations with parental C1498, C1498-m157wt and C1498-m157-N178,187,213,267Q are shown in Fig. 6A. For the mixture containing parental C1498 cells, only Ly49H staining is detected on the $CFSE^+$ subset as expected (Fig 6A, left column; $CFSE^+$ gate not shown). However, even at the earliest assessable time point, Ly49H and *wt*-m157 show a clear interaction as detected by the presence of mAb 6D5 reactivity on the Ly49H-expressing ($CFSE^+$) HD12 cells, most likely reflecting transfer of m157 since the gating reflects only single-cell events in this analysis. By 185 min, the m157 staining on HD12 cells in this mixture is lost (Fig. 6A, middle column). In contrast, despite abundant surface expression for both m157 and Ly49H in the mixture containing C1498-m157-N178,187,213,267Q, the HD12 cells show reduced staining for m157 with mAb 6D5 to a near background level (Fig. 6A, right column). Graphical depiction of the mean fluorescence intensity (MFI) for anti-m157 staining on $CFSE^+$ HD12 cells shows that over the initial 45 min of coincubation, Ly49H and *wt*-m157 are physically associated to a greater degree than occurs for Ly49H and unglycosylated m157 (Fig. 6B). It is also noteworthy that the decrease in MFI for *wt*-m157 on C1498 cells (58.6% reduction) is greater than that observed for the unglycosylated variant (2.3% reduction), reflecting either the greater physical loss of the *wt*-m157 due to Ly49H binding/transfer, or a faster rate of recovery for the unglycosylated m157 variant displayed at the surface. However, previous experiments assessing the PI-PLC susceptibility of all the glycosylation variants of m157 did not reveal significant differences in cell surface recovery of m157 following treatment (data not shown). Together with the finding above that m157-N178,187,213,267Q cannot be coimmunoprecipitated after 40 min coincubation with Ly49H, these results further indicate that the lack of glycosylation on m157 leads to a reduced stability of interaction with Ly49H.

Confocal microscopy reveals physical transfer of wt-m157, but not unglycosylated m157, to Ly49H-expressing cells

It is well established that cell surface proteins and membrane fragments may be transferred between immune cells following contact (trogocytosis) [24,36,37]. Human and mouse NK cells acquire cognate MHC class I molecules *in vitro* and *in vivo* [26,38]. To verify that the flow cytometry results depicted in Fig. 6A reflected the physical transfer of m157 to $Ly49H^+$ HD12 cells, we examined dual-labeled cell mixtures by confocal microscopy. Initially, CFSE-labeled HD12 cells were coincubated with C1498-m157wt or C1498-m157-N178,187,213,267Q cells labeled with Cy-5-6D5 (anti-m157), and examined over 30 min at 2-min intervals. As shown in Fig. 6C for HD12-C1498-m157wt cells, there is clear transfer of m157 staining to the HD12 cells during 25 minutes of coincubation. We detected little or no m157 staining of HD12 cells when coincubated with C1498 cells expressing unglycosylated m157 at any time point. Coincubation of C1498-m157wt cells with control BWZ cells, which do not express Ly49H receptor, did not reveal m157 ligand transfer; also, Cy-5-labeled isotype control mAb did not stain HD12 cells (or C1498-m157wt cells), indicating specificity for Ly49H and m157, respectively (data not shown).

Next we incubated CFSE-labeled HD12 cells with a mixture of C1498-m157wt cells and C1498-m157-N178,187,213,267Q cells in the same sample. The C1498 cells expressing unglycosylated m157 were labeled with PKH-26 to distinguish them during microscopy (dark pink-stained cells, Fig. 6D). The cells were allowed to interact for 15 min prior to the addition of Cy-labeled 6D5 and then imaged every 2 min, maintaining the temperature at 37 °C. Only the conjugates involving C1498-m157wt cells (red) show clear transfer of m157 staining to HD12 cells; transfer of unglycosylated m157 was not observed over the duration of coincubation (Fig. 6D). These data show that m157 is physically transferred to Ly49H-expressing cells following cellular interaction, as has been described for the MHC class I ligands of other members of the Ly49 receptor family [25,26]. Moreover, as was observed for optimal Ly49H-m157 coimmunoprecipitation, glycosylation of m157 is required for Ly49H-mediated trogocytosis at a level that is detectable by confocal microscopy.

Discussion

For classical lectins, N-linked glycans are critical determinants for receptor recognition [5]. For some proteins, N-linked glycans are important for folding and/or exit from the ER, but not for their biological function [39,40]. For other protein ligands, glycosylation may stabilize discrete conformations, as has been postulated for one or more N-linked glycans of m157 (e.g., N178) [41]. We observed that the pattern of expression for m157 in transduced or MCMV-infected cells differs among host cell types, both in the molecular mass and in the relative abundance of individual m157 isoforms (Figs. 1B and 2C). We determined that the majority, if not all, of this molecular variability is due to N-linked glycosylation.

All N-glycosylation variants of m157 were expressed at the surface and recognized by multiple m157-specific reagents in both myeloid and fibroblast cell types (Figs. 3A, 3B, Suppl. Fig.1 and data not shown). However, progressive loss of N-linked glycans had a dramatic effect on overall cellular abundance of m157, particularly for the triple and quadruple (completely unglycosylated) mutants (Fig. 3B). Variably glycosylated m157 isoforms are not differentially secreted/shed into culture supernatants (Fig. 3C). It has been reported that incorrect or incomplete N-glycosylation of some proteins targets them for degradation in a process requiring poly-ubiquitination [42, 43]. However, we determined that N-glycosylation does not grossly alter subcellular localization, ubiquitination (ubiquitinated m157 is not detected in transduced cells) or proteasomal/lysosomal degradation of m157 (Suppl. Fig. 1 and data not shown). Lack of all N-linked glycans decreases the half-life of m157 expressed in C1498 cells following cyclohexamide treatment

(Suppl Fig. 2), a finding that may partially explain why we were unable to detect significant differences in m157 turnover, since measurements of m157 degradation in the presence of proteasome inhibition and m157-ubiquitination were made prior to 24 hrs. Even considering this decreased half-life, we cannot rule out another effect of cumulative N-glycosylation of m157 that regulates the rate of posttranslational processing (synthesis) or conformational stability. A similar reduction in overall protein abundance associated with the loss of N-linked glycosylation has been reported for the NMDA receptor NR1 [44] and TTYH2, a member of Tweety family of Cl^- channels [45]. It is clear that differential N-glycosylation accounts for the multiplicity of m157 isoforms across all transduced or MCMV-infected cell types, since treatment with PNGase F collapses all isoforms to a common species at ~32 kDa (Figs. 2B, 2C and 3B).

A published crystal structure for m157 produced in Sf9 insect cells shows that all four predicted N-glycosylation sites are found within the membrane-proximal α3 domain, but that only N178 and N187 were glycosylated. The glycans at position N178 were predicted to provide stabilization for the overall m157 structure through contacts with the α1/α2 platform [41]. Our data clearly show that all four putative N-glycosylation sites are utilized in mouse cells (Fig. 3B), and no single site appears to be critical for cell surface expression, stability, or function of m157. Thus, assuming that all four sites are utilized in all cells, the differential pattern of m157 isoforms observed in transduced and MCMV-infected cells may arise from the particular oligosaccharide moieties at each site. More detailed studies are required to determine whether differentially glycosylated m157 isoforms are displayed at the cell surface among cell types, or differentially recognized by $Ly49H^+$ (or $Ly49I^{129+}$) NK cells—analyses complicated by the low abundance of surface m157 among MCMV-infected cells (C.A.F. and J.W.H., unpublished observation and [31]). Potentially, differential glycosylation at these four sites may impact viral fitness and/or the host immune response among MCMV-infected tissues, as has been clearly shown for influenza virus, HIV, and other pathogenic viruses (reviewed in [46]).

For transduced BWZ.36 reporters expressing Ly49H (HD12 cells) or $Ly49I^{129}$ (HI-129 cells), functional recognition of m157 expressed on transduced C1498, P815, or 3T3 fibroblast cells occurs independently of N-glycosylation (Fig. 4A and Suppl. Fig. 3). Similarly, $Ly49H^+$ NK cells are activated by all of these m157 N-glycosylation variants (Fig. 4B–D), although the extent of Ly49H receptor downregulation was consistently lower for interactions with fully unglycosylated m157 (Fig. 4B, C). This likely reflected a diminished stability of binding, similar to previous observations for selected m157 mutants that fail to activate HD12 cells [29]. Consistent with this interpretation was the finding that 3D10-mediated coimmunoprecipitation of unglycosylated m157 was dramatically reduced between 10 and 40 min coincubation of HD12 cells with C1498-m157-N178,187,213,267Q cells (Fig. 5A), suggesting that even minimal glycosylation of m157 (e.g. only at position N267 for the triple mutant) affords enhanced stability of binding in this receptor-ligand interaction. Although it is possible that the loss of glycosylation at multiple sites reduces the conformational stability of m157, and thus the proportion of ligand that is available for binding to Ly49H, the kinetic data suggest that Ly49H interaction with unglycosylated m157 has a reduced overall stability, most consistent with a faster off-rate (Fig. 5B, 5C), although more formal binding studies are required to verify this possibility. This is consistent with the observation that isolated mutation of N178, alone or in combination with N187Q, has no detectable effect on the conformational stability of m157 as predicted from the crystal structure [41]. Among the m157 sequences reported to GenBank, N187, N213, and N267 all are conserved in all m157 variants, whereas N187 is not, and there is no correlation between the presence of N187 and binding to Ly49H among the m157 variants with known Ly49H-binding capacity [10]. Furthermore, it is apparent that, like the promiscuity with which NKG2D binds its ligands, Ly49H is tolerant to mutations in m157

that would be predicted to compromise an induced fit structural interaction [29,41]. For m157 variants that are expressed at the cell surface, loss of Ly49H binding and/or activation is seen only after accumulation of multiple nonconservative mutations [10], or for isolated mutations in buried residues that may dramatically alter its Ly49H-binding conformation [29]. Thus, the 'rigid adaptation' model proposed for NKG2D-ligand interactions may be generally applicable for the group V NK cell lectin-like receptors [47].

The finding that Ly49H-expressing HD12 cells become transiently $m157^+$ when coincubated with C1498-m157wt cells is consistent with what has been reported for inhibitory Ly49 receptors (and human KIR) binding MHC I ligands, whereby the physical transfer of ligand onto receptor-expressing NK cells occurs [24–26,38,48]. Trogosytosis has also been described for the activating NKG2D receptor [27,28]. Our results in Fig. 6 indicate that N-glycosylation of m157 is required for efficient transfer of m157 onto HD12 cells. Importantly, for both HD12 cells and $Ly49H^+$ NK cells, physical transfer of m157 at levels detectable by flow cytometry, or co-immunoprecipitation followed by western blotting, is not required for signaling, since all N-glycosylation mutants were capable of activating Ly49H-expressing cells as efficiently as *wt*-m157 (Fig. 4 and data not shown). However, considering that C1498 cells expressing unglycosylated m157 also are less efficient in driving Ly49H receptor downregulation, we are interested to determine whether Ly49H signaling may be uncoupled from both m157 transfer and Ly49H receptor internalization. Thus, glycosylation of Ly49 receptor ligands expressed at low density, such as m157 on MCMV-infected cells, may assist in promoting efficient receptor aggregation, which may in turn afford sustained receptor signaling. Future studies using recombinant MCMV encoding the m157-N178,187,213,267Q variant will be required to address this hypothesis.

Consistent with other group V CLR-ligand interactions, Ly49H is able to bind m157 with reduced or no N-linked carbohydrates, and this interaction results in robust NK cell activation. This observation is striking, given that fully unglycosylated m157 shows a reduced stability of interaction with Ly49H as assessed biochemically and on live cells. Glycosylation is also important for physical transfer of m157 to Ly49H-expressing cells. While this large group of immune cell receptors appear to be lectins only in name, they may retain some carbohydrate-recognition capacity that serves a more subtle contribution to specificity, as was found for Ly49A [49], and/or overall avidity. It is evident that the functional interactions of Ly49 receptors and their ligands are remarkably tolerant to multiple amino acid substitutions and post-translational modifications. This manifests as ligand promiscuity for these lectin-like receptors, and likely reflects not only the need to keep pace with ongoing dynamic evolution of MHC class I and related structures, but also the need for cooperation among them in regulating the activation threshold for potent immune cells.

Materials and methods

Mice

BALB/c, C57BL/6, (NCI-Frederick, Frederick, MD) and B6.129S7-*Rag1*^{tmMom}/J (*RAG1*-deficient) mice used for propagation of virulent MCMV virus or as a source for fresh NK cells were maintained in the University of Iowa Animal Care Unit barrier facility. Experiments using mice were conducted according to protocols approved by the University of Iowa Animal Care and Use Committee.

Cell Lines, MCMV infection, Retroviral transduction, and Flow Cytometry

The retroviral transduction system including the pMX vectors, Platinum-E (PLAT-E) packaging cell line, BWZ.36 cells harboring an inducible NFAT-lacZ reporter cassette, and

the derivative Ly49H reporter line (HD12 cells) have been described previously [14]. The Ly49HI^{129} and Ly49HI^{B6} cell lines were generously provided by Wayne Yokoyama (HHMI at Washington University, St. Louis, MO). All BWZ.36-derived cell lines and P815 (DBA/2 mastocytoma)-derived cell lines were maintained in RPMI 1640 (GIBCO/Invitrogen, Carlsbad, CA) supplemented with 10% fetal bovine serum (FBS; Hyclone, Logan, UT), 2 mM L-glutamine, and 10 mM Hepes ("R10"). NIH-3T3, 3T12 fibroblasts and C1498 (C57BL/6J myeloid leukemia) cells and transduced derivatives were maintained in complete Dulbeco's Modified Eagle's Medium (DMEM/high glucose, GIBCO/Invitrogen, Carlsbad, CA) supplemented with 10% FBS, 1 mM (sodium) pyruvate, 2 mM L-glutamine, and 10 mM Hepes ("D10") plus 50 μM 2-mercaptoethanol. The DC2.4 dendritic cell line (kindly provided by Kenneth Rock, University of Massachusetts Medical School, Worcester, MA and the Dana-Farber Cancer Institute, Boston, MA) was cultured in Hepes-buffered R10 plus sodium pyrvutate.

MCMV (Smith or K181-derived RM4503.3 [50] strains) passaged *in vivo* (BALB/c mice) and prepared from salivary gland was used to infect 3T12 fibroblasts at a low multiplicity of infection (m.o.i.) to expand viral stocks for use in *in vitro* infections. This fibroblast single-passage MCMV was mixed with the indicated host cell lines at a m.o.i = 10 in a low volume. After 90 minutes adsorption in complete medium supplemented with 2% FCS, complete medium (e.g., R10 or D10) was added and the infections were incubated for 12–24 hr at 37 °C/5% CO_2.

Wild-type (*wt*) and mutant m157 cDNA constructs were directionally subcloned into the *Bam*HI and *Not*I sites of the pMX-Puro retroviral vector (pMX vectors and PLAT-E cells kindly provided by T. Kitamura, University of Tokyo). Transduced cells were surface stained with Cy5-conjugated monoclonal antibodies (mAbs) specific for m157: 6D5 [29] or 6H121[31]. Fluorescently labeled cells were analyzed on a FACSCalibur flow cytometer (BD Biosciences, San Jose, CA, USA) and the data processed using FlowJo software (version 8.4.6, Tree Star Inc., Ashland, OR, USA).

Site-directed mutagenesis

PCR mutagenesis of m157 was performed using a site-directed mutagenesis kit according to the manufacture's standard protocol (Stratagene, Cedar Creek, TX). Asparagine in the consensus sequence for N-glycosylation, Asn-X-Ser/Thr, was mutated to glutamine by altering the Asn codon (**bold type**) in the following primers: N178Q, 5'-CAACTCGCATACATG**CAG**GCGACCGAAGTCGAG; N187Q, 5'-GTCGAGTTCTGGTAC **CAG**ACGACCGGCTTGACC; N213Q, 5'-GAATTATCCTTGAACACT**CAG**AGCTCTGCGATC GTTACTG; N267Q, 5'-CGAAACGCGTGCCTGTC**CAG**ATCAGCTCTTCGAAATG.

CPRG Assay for β-galactosidase activity

Activation of the inducible *lacZ* reporter line, BWZ.36 [51], and the derivative lines HD12 (expressing Ly49H), HI129 and HIB6 (expressing chimeric Ly49H-Ly49I receptors) coupled to the DAP12 signaling adaptor was assessed as previously described [29]. Conversion of the colorimetric chlorophenol red β-D-galactopyranoside (CPRG) substrate was quantitatively determined at several points during the linear phase of enzymatic activity by measuring the absorbance at 575 nm (635 nm reference) using a μ-Quant plate reader and K.C.-Jr. software package (Bio-Tek Instruments, Inc., Winooski, VT). Results are shown as a percentage of maximal stimulation obtained upon culturing each reporter cell line alone with 5 ng/mL phorbol-myristate acetate (PMA) and 1 μM ionomycin.

Western blot analysis and coimmunoprecipitation

Western blot analysis was performed as previously described using m157-specific mAb 6H121 [29,31]. Equal loading was controlled by reversible staining of the membrane with Ponceau S solution and with antibodies to actin (Sigma-Aldrich, St. Louis, MO). For Ly49H-m157 coimmunoprecipitation analysis, HD12 cells expressing Ly49H receptor were incubated with stimulator cells expressing m157 (*wt*-m157 or one of the seven N-glycosylation mutants; reporter:stimulator = 1:2) for 10 and 40 min; immunoprecipitation using anti-Ly49H mAb 3D10 and detection by western blotting for m157 with mAb 6H121were performed as described [29]. Note that in the absence of a reagent to detect Ly49H in western blot analysis, we verified Ly49H expression on HD12 cells by flow cytometry before each experiment.

Analysis of N-linked Glycosylation and GPI-linkage

The extent of N-linked oligosaccharide modification for m157 was determined by treatment of cellular lysates with peptide N-glycosidase F (PNGase F) or Endoglycosidase H (Endo H) (New England BioLabs, Ipswich, MA) according to the manufacturer's instructions. Samples were incubated for 1 hr at 37°C and then analyzed by western blotting for detection of m157 as described above.

GPI linkage of m157 mutants was assessed by treatment of 2×10^6 cells with 2U of phosphatidylinositol-specific phospholipase C (PI-PLC; Invitrogen; Eugene, OR) in 0.5 ml of complete medium. After 1 hr of incubation at 37 °C, cells were pelleted by centrifugation at 600×*g* for 5 min and 10 μl of supernatant were diluted in sample buffer and analyzed by western blot.

Flow cytometric analysis of the Ly49H-m157 interactions in HD12-C1498 cell mixtures

Ly49H-expressing HD12 cells were stained with 1 μM carboxyfluorescein succinamidyl ester (CFSE; Sigma-Aldrich, St. Louis, MO) for 5 min at 37 °C prior to coincubation with stimulator C1498 cell lines. CFSE labeling was terminated by addition of an equal volume of FBS followed by washing in PBS + 5% FBS. Labeled HD12 cells were incubated with stimulator cells expressing *wt*-m157 or the fully unglycosylated mutant, m157-N178, 187, 213, 267N (reporter:stimulator = 1:1) in R10 medium for times ranging from 5 to 185 min. The 5 min time point represents cells mixed together and then immediately centrifuged and processed for staining. Other samples were harvested after an additional 10, 40, or 180 min at 37 °C and 5% CO_2. At the indicated times for coincubation, cell mixtures were transferred into PBS/5% FBS/0.2% sodium azide, centrifuged and then stained for Ly49H (mAb 3D10-R-phycoerythrin) and m157 (mAb 6D5-allophycocyanin) for 5 min at room temperature then washed and fixed with BD FACS™ Lysing Solution (BD Biosciences, San Jose CA) according to package directions. Samples were analyzed by flow cytometry as described above.

Intracellular cytokine staining of fresh NK cells

Intracellular staining was performed as in [14] with modification. Freshly isolated B6.RAG1$^{-/-}$ splenocytes were co-cultured for 6 hr with m157-transduced C1498, P815 or 3T12 cells (1:1 for MIP-1α or 8:1 for INF-γ) in a 48-well plate (10^6 total cells/well; brefeldin A (10 μg/ml) was added for the final 5 hr to allow for accumulation of intracellular cytokines. Cells were collected with Versene and stained with anti-NK1.1-FITC (mAb PK136), and Cy5-conjugated anti-Ly49H mAb 3D10 (GE Healthcare Piscataway, NJ, USA) along with unlabeled mAb 2.4G2 to block non-specific Fc receptor binding. Following fixation and permeablization, cells were incubated with anti-MIP-1α-PE (R&D Systems

clone 39624), or anti IFN-γ-PE-Cy7 (BD PharMingen, San Diego, CA, USA; clone XMG1.2), washed and then analyzed on a FACSCalibur flow cytometer as above.

Chromium release assay for NK cell cytotoxicity

NK cell cytotoxicity *in vitro* was assessed by standard ^{51}Cr-release assay as described [52]. Fresh B6.RAG1$^{-/-}$ splenocytes were used as a source for NK cells; the Ly49H^{+} subset was ~63% of the NK1.1^{+} splenocytes. Parental C1498, m157-expressing C1498 cells, or YAC-1 cellular targets (5×10^{3}) were labeled with 10 $_{\mu}$Ci of ^{51}Cr (NEN, Boston, Mass.), washed and mixed with NK cells at effector to target (E:T) ratios ranging from 3:1-to100:1(in triplicate). Killing activity is expressed as the percentage of specific ^{51}Cr release: % cytotoxicity = [(experimental ^{51}Cr release− spontaneous ^{51}Cr release)/(maximum ^{51}Cr release −spontaneous ^{51}Cr release)]×100. For the control experiments, the target cells were incubated either in the culture medium alone to determine the spontaneous release or in 1% acetic acid to define the maximum ^{51}Cr release. The spontaneous release was always <10% of the maximum release. Anti-m157 mAb 6D5 (1 μg/mL or 10 μg/mL) was added to control for specificity of Ly49H-mediated killing.

Generation of soluble m157-Fc proteins and use in flow cytometric binding assays

The CP197 construct containing the Smith m157-Fc behind the CD150L sequence cloned in the CDM8 vector [8] was kindly provided by Dr L. Lanier (University of California, San Francisco, CA USA). Soluble unglycosylated m157-Fc fusion proteins were generated similarly, replacing the *wt*-m157 cDNA sequence with a PCR fragment amplified from the pMX-Puro-m157-N178,187,213,267Q construct (minus the predicted leader sequence and truncated before the GPI anchor motif) using the following primers containing the *Xho*I recognition sequence (m157FcF11: TATATCTCGAGATTTTCAATCCTGATCCTGA; and m157FcR1: ATTCTCGAGACGGTTGACATTCCCTTTCC). Both *wt*-m157 and unglycosylated m157 are fused at the same junction to the human Fc portion of IgG. Soluble fusion proteins were expressed by transient transfection in COS-7 cells using FuGene 6 transfection reagent (Roche Diagnostics). In some experiments, soluble m157-Fc proteins were used as concentrated (~10x) COS-7 cell supernatants. Secreted proteins were also purified from supernatants using protein G Nunc ProPur™ kit with mini spin columns (Thermo Fisher Scientific Inc, Rochester, NY).

Purified m157-Fc proteins or concentrated supernatants were labeled using the Zenon™ Human IgG labeling reagents that are goat, Alexa-Fluor-647–labeled, Fab fragments directed against the Fc portion of human IgG. Ly49H-expressing HD12 cells were incubated with 100 μl of Alexa-fluor 647-labeled m157wt-Fc or m157-N178,187,213,267Q–Fc protein containing supernatants for 15 min at room temperature. For kinetic dissociation experiments, the volume of COS-7 cell supernatants containing m157-Fc proteins that provided equivalent and maximal staining of HD12 cells was initially determined empirically (ratio for *wt*-m157-Fc:m157-N178,187,213,267Q-Fc ~1:2). Samples were washed with BSA containing PBS and after gentle resuspension anti-m157 6D5 (400μg/ml) or anti-Ly49H 3D10 (400μg/ml) was added and cells were incubated at room temperature for the duration of the experiment. Samples were analyzed every 10 min by FACSCalibur flow cytometer as described above.

Confocal Microscopy

Parental and m157-expressing C1498 cells were grown on glass coverslips covered with 1% poly-lysine. Cells were fixed in 4% paraformaldehyde in PBS for 20 min at room temperature, washed twice with PBS and incubated in ice-cold digitonin permeablization buffer (0.005% digitonin, 0.3 M sucrose, 0.1M KCl, 2.5 mM $MgCl_2$, 1mM EDTA, 10mM HEPES pH 6.9) for 20 min at 4 °C. Cells were washed and blocked with PBS containing 2%

bovine serum + 10% goat serum at room temperature for 30 min and then incubated with 6D5 (50 μg/ml) or anti-giantin (1:1000; Covance; Berkeley, CA) antibodies for 30 min at room temperature. After washing in PBS 4 times, cells were incubated with a mixture of secondary anti-mouse conjugated with Alexa-488 (1:500) and anti-rabbit conjugated with Alexa-556 (1:500) for 1 hour at room temperature, and then washed again with PBS.

For confocal imaging of live cells, HD12 cells were labeled with 1 μM CFSE for 5 min at 37°C. In some experiments, C1498-m157-N178,187,213,267N cells were labeled with 2 μM PKH-26 for 5 min at room temperature. Ligand expressing cells were mixed with receptor expressing cells (1:1) in final concentration of 2×10^6/mL on a glass bottom culture dish and cell mixture was incubated for 5 min at 37°C. A Zeiss Heating Stage was used to maintain cells at a constant 37°C during incubation periods and imaging. 6D5-Cy5 antibodies were added (1:100) and live cell imaging was performed by confocal laser scanning microscopy using a Zeiss LSCM 510 (Carl Zeiss, Inc., Thornwood, NY) and ×63 oil immersion objective.

Supplementary Material

Refer to Web version on PubMed Central for supplementary material.

Abbreviations

CLR	C-type lectin receptor
CPRG	chlorophenol red-β-D-galactopyranoside
MCMV	murine cytomegalovirus
MIP-1α	macrophage inflammatory protein type 1a, [also, CCL3]

Acknowledgments

The authors would like to thank Mike Knudson, Tom Waldschmidt, Kevin Legge and Oskar Rohklin (University of Iowa) for reagents, helpful discussions, and/or critical review of the manuscript, and A. Menon (Weill Cornell Medical College) for insight on GPI anchor biochemistry. Expert graphics and administrative support was provided by Joel Carl and Carla Hartl, respectively. This work was supported in part by National Institutes of Health R56 AI063226-01.

References

1. Lanier LL. Evolutionary struggles between NK cells and viruses. Nat Rev Immunol. 2008; 8:259–268. [PubMed: 18340344]
2. Scalzo AA, Yokoyama WM. Cmv1 and natural killer cell responses to murine cytomegalovirus infection. Curr Top Microbiol Immunol. 2008; 321:101–122. [PubMed: 18727489]
3. Yokoyama WM. Specific and non-specific natural killer cell responses to viral infection. Adv Exp Med Biol. 2005; 560:57–61. [PubMed: 15932020]
4. Orange JS. Human natural killer cell deficiencies and susceptibility to infection. Microbes & Infection. 2002; 4:1545–1558. [PubMed: 12505527]
5. Zelensky AN, Gready JE. The C-type lectin-like domain superfamily. Febs J. 2005; 272:6179–6217. [PubMed: 16336259]
6. Yokoyama WM, Plougastel BF. Immune functions encoded by the natural killer gene complex. Nat Rev Immunol. 2003; 3:304–316. [PubMed: 12669021]
7. Kumar V, McNerney ME. A new self: MHC-class-I-independent natural-killer-cell self-tolerance. Nat Rev Immunol. 2005; 5:363–374. [PubMed: 15841099]

8. Arase H, Mocarski ES, Campbell AE, Hill AB, Lanier LL. Direct recognition of cytomegalovirus by activating and inhibitory NK cell receptors.[comment]. Science. 2002; 296:1323–1326. [PubMed: 11950999]
9. Scalzo AA, Corbett AJ, Rawlinson WD, Scott GM, Degli-Esposti MA. The interplay between host and viral factors in shaping the outcome of cytomegalovirus infection. Immunol Cell Biol. 2007; 85:46–54. [PubMed: 17146464]
10. Voigt V, Forbes CA, Tonkin JN, Degli-Esposti MA, Smith HRC, Yokoyama WM, Scalzo AA. Murine cytomegalovirus m157 mutation and variation leads to immune evasion of natural killer cells. Proc Natl Acad Sci. 2003; 100:13483–13488. [PubMed: 14597723]
11. Cerwenka A, Lanier LL. NKG2D ligands: unconventional MHC class I-like molecules exploited by viruses and cancer. Tissue Antigens. 2003; 61:335–343. [PubMed: 12753652]
12. Voigt S, Mesci A, Ettinger J, Fine JH, Chen P, Chou W, Carlyle JR. Cytomegalovirus evasion of innate immunity by subversion of the NKR-P1B:Clr-b missing-self axis. Immunity. 2007; 26:617–627. [PubMed: 17462921]
13. Lenac T, Arapovic J, Traven L, Krmpotic A, Jonjic S. Murine cytomegalovirus regulation of NKG2D ligands. Med Microbiol Immunol. 2008; 197:159–166. [PubMed: 18259774]
14. Smith HR, Heusel JW, Mehta IK, Kim S, Dorner BG, Naidenko OV, Iizuka K, Furukawa H, Beckman DL, Pingel JT, Scalzo AA, Fremont DH, Yokoyama WM. Recognition of a virus-encoded ligand by a natural killer cell activation receptor. Proc Natl Acad Sci U S A. 2002; 99:8826–8831. [PubMed: 12060703]
15. Scalzo AA, Fitzgerald NA, Simmons A, La Vista AB, Shellam GR. Cmv-1, a genetic locus that controls murine cytomegalovirus replication in the spleen. J Exp Med. 1990; 171:1469–1483. [PubMed: 2159050]
16. Brown MG, Dokun AO, Heusel JW, Smith HR, Beckman DL, Blattenberger EA, Dubbelde CE, Stone LR, Scalzo AA, Yokoyama WM. Vital involvement of a natural killer cell activation receptor in resistance to viral infection. Science. 2001; 292:934–937. [PubMed: 11340207]
17. Daniels KA, Devora G, Lai WC, O'Donnell CL, Bennett M, Welsh RM. Murine cytomegalovirus is regulated by a discrete subset of natural killer cells reactive with monoclonal antibody to Ly49H. J Exp Med. 2001; 194:29–44. [PubMed: 11435470]
18. Lee SH, Girard S, Macina D, Busa M, Zafer A, Belouchi A, Gros P, Vidal SM. Susceptibility to mouse cytomegalovirus is associated with deletion of an activating natural killer cell receptor of the C-type lectin superfamily.[comment]. Nature Genetics. 2001; 28:42–45. [PubMed: 11326273]
19. Abi-Rached L, Parham P. Natural selection drives recurrent formation of activating killer cell immunoglobulin-like receptor and Ly49 from inhibitory homologues. J Exp Med. 2005; 201:1319–1332. [PubMed: 15837816]
20. Arase H, Lanier LL. Virus-driven evolution of natural killer cell receptors. Microbes & Infection. 2002; 4:1505–1512. [PubMed: 12505522]
21. Sun JC, Lanier LL. Tolerance of NK cells encountering their viral ligand during development. J Exp Med. 2008; 205:1819–1828. [PubMed: 18606858]
22. Deng L, Mariuzza RA. Structural basis for recognition of MHC and MHC-like ligands by natural killer cell receptors. Semin Immunol. 2006; 18:159–166. [PubMed: 16737824]
23. Strong RK. Asymmetric ligand recognition by the activating natural killer cell receptor NKG2D, a symmetric homodimer. Mol Immunol. 2002; 38:1029–1037. [PubMed: 11955595]
24. Hudrisier JE. What is trogocytosis and what is its purpose? Nat Immunol. 2003; 4:815. [PubMed: 12942076]
25. Sjostrom A, Eriksson M, Cerboni C, Johansson MH, Sentman CL, Karre K, Hoglund P. Acquisition of external major histocompatibility complex class I molecules by natural killer cells expressing inhibitory Ly49 receptors. J Exp Med. 2001; 194:1519–1530. [PubMed: 11714758]
26. Zimmer J, Ioannidis V, Held W. H-2D ligand expression by Ly49A+ natural killer (NK) cells precludes ligand uptake from environmental cells: implications for NK cell function. J Exp Med. 2001; 194:1531–1539. [PubMed: 11714759]
27. Roda-Navarro P, Vales-Gomez M, Chisholm SE, Reyburn HT. Transfer of NKG2D and MICB at the cytotoxic NK cell immune synapse correlates with a reduction in NK cell cytotoxic function. Proc Natl Acad Sci U S A. 2006; 103:11258–11263. [PubMed: 16849432]

28. McCann FE, Eissmann P, Onfelt B, Leung R, Davis DM. The activating NKG2D ligand MHC class I-related chain A transfers from target cells to NK cells in a manner that allows functional consequences. J Immunol. 2007; 178:3418–3426. [PubMed: 17339436]
29. Davis AH, Guseva NV, Ball BL, Heusel JW. Characterization of murine cytomegalovirus m157 from infected cells and identification of critical residues mediating recognition by the NK cell receptor Ly49H. J Immunol. 2008; 181:265–275. [PubMed: 18566392]
30. Gasteiger E, G A, Hoogland C, Ivanyi I, Appel RD, Bairoch A. ExPASy: the proteomics server for in-depth protein knowledge and analysis. Nucleic Acids Res. 2003; 31:3784–3788. [PubMed: 12824418]
31. Tripathy SK, Smith HRC, Holroyd EA, Pingel JT, Yokoyama WM. Expression of m157, a Murine Cytomegalovirus-Encoded Putative Major Histocompatibility Class I (MHC-I)-Like Protein, Is Independent of Viral Regulation of Host MHC-I. J Virol. 2006; 80:545–550. [PubMed: 16352579]
32. Linstedt AD, Hauri HP. Giantin, a novel conserved Golgi membrane protein containing a cytoplasmic domain of at least 350 kDa. Mol Biol Cell. 1993; 4:679–693. [PubMed: 7691276]
33. Dorner BG, Smith HR, French AR, Kim S, Poursine-Laurent J, Beckman DL, Pingel JT, Kroczek RA, Yokoyama WM. Coordinate expression of cytokines and chemokines by NK cells during murine cytomegalovirus infection. J Immunol. 2004; 172:3119–3131. [PubMed: 14978118]
34. Smith HR, Chuang HH, Wang LL, Salcedo M, Heusel JW, Yokoyama WM. Nonstochastic coexpression of activation receptors on murine natural killer cells. J Exp Med. 2000; 191:1341–1354. [PubMed: 10770801]
35. Dokun AO, Kim S, Smith HR, Kang HS, Chu DT, Yokoyama WM. Specific and nonspecific NK cell activation during virus infection. Nature Immunology. 2001; 2:951–956. [PubMed: 11550009]
36. Ahmed KA, Munegowda MA, Xie Y, Xiang J. Intercellular trogocytosis plays an important role in modulation of immune responses. Cell Mol Immunol. 2008; 5:261–269. [PubMed: 18761813]
37. Caumartin J, Lemaoult J, Carosella ED. Intercellular exchanges of membrane patches (trogocytosis) highlight the next level of immune plasticity. Transpl Immunol. 2006; 17:20–22. [PubMed: 17157208]
38. Carlin LM, Eleme K, McCann FE, Davis DM. Intercellular transfer and supramolecular organization of human leukocyte antigen C at inhibitory natural killer cell immune synapses. J Exp Med. 2001; 194:1507–1517. [PubMed: 11714757]
39. Helenius A, Aebi M. Roles of N-linked glycans in the endoplasmic reticulum. Annu Rev Biochem. 2004; 73:1019–1049. [PubMed: 15189166]
40. Helenius A. How N-linked oligosaccharides affect glycoprotein folding in the endoplasmic reticulum. Mol Biol Cell. 1994; 5:253–265. [PubMed: 8049518]
41. Adams EJ, Juo ZS, Venook RT, Boulanger MJ, Arase H, Lanier LL, Garcia KC. Structural elucidation of the m157 mouse cytomegalovirus ligand for Ly49 natural killer cell receptors. Proc Natl Acad Sci. 2007; 104:10128–10133. [PubMed: 17537914]
42. Jones J, Krag SS, Betenbaugh MJ. Controlling N-linked glycan site occupancy. Biochim Biophys Acta. 2005; 1726:121–137. [PubMed: 16126345]
43. Lederkremer GZ, Glickman MH. A window of opportunity: timing protein degradation by trimming of sugars and ubiquitins. Trends Biochem Sci. 2005; 30:297–303. [PubMed: 15950873]
44. Everts I, Villmann C, Hollmann M. N-Glycosylation is not a prerequisite for glutamate receptor function but Is essential for lectin modulation. Mol Pharmacol. 1997; 52:861–873. [PubMed: 9351977]
45. He Y, Ramsay AJ, Hunt ML, Whitbread AK, Myers SA, Hooper JD. N-glycosylation analysis of the human Tweety family of putative chloride ion channels supports a penta-spanning membrane arrangement: impact of N-glycosylation on cellular processing of Tweety homologue 2 (TTYH2). Biochem J. 2008; 412:45–55. [PubMed: 18260827]
46. Vigerust DJ, Shepherd VL. Virus glycosylation: role in virulence and immune interactions. Trends Microbiol. 2007; 15:211–218. [PubMed: 17398101]
47. McFarland BJ, Strong RK. Thermodynamic analysis of degenerate recognition by the NKG2D immunoreceptor: not induced fit but rigid adaptation. Immunity. 2003; 19:803–812. [PubMed: 14670298]

48. Andersson KE, Williams GS, Davis DM, Hoglund P. Quantifying the reduction in accessibility of the inhibitory NK cell receptor Ly49A caused by binding MHC class I proteins in cis. Eur J Immunol. 2007; 37:516–527. [PubMed: 17236237]

49. Lian RH, Freeman JD, Mager DL, Takei F. Role of conserved glycosylation site unique to murine class I MHC in recognition by Ly-49 NK cell receptor. J Immunol. 1998; 161:2301–2306. [PubMed: 9725224]

50. van Den Pol AN, Mocarski E, Saederup N, Vieira J, Meier TJ. Cytomegalovirus cell tropism, replication, and gene transfer in brain. Journal of Neuroscience. 1999; 19:10948–10965. [PubMed: 10594076]

51. Karttunen J, Shastri N. Measurement of Ligand-Induced Activation in Single Viable T Cells Using the lacZ Reporter Gene. Proceedings of the National Academy of Sciences. 1991; 88:3972–3976.

52. Shey MR, Ballas ZK. Assessment of natural killer (NK) and NKT cells in murine spleens and livers. Methods Mol Biol. 2008; 447:259–276. [PubMed: 18369924]

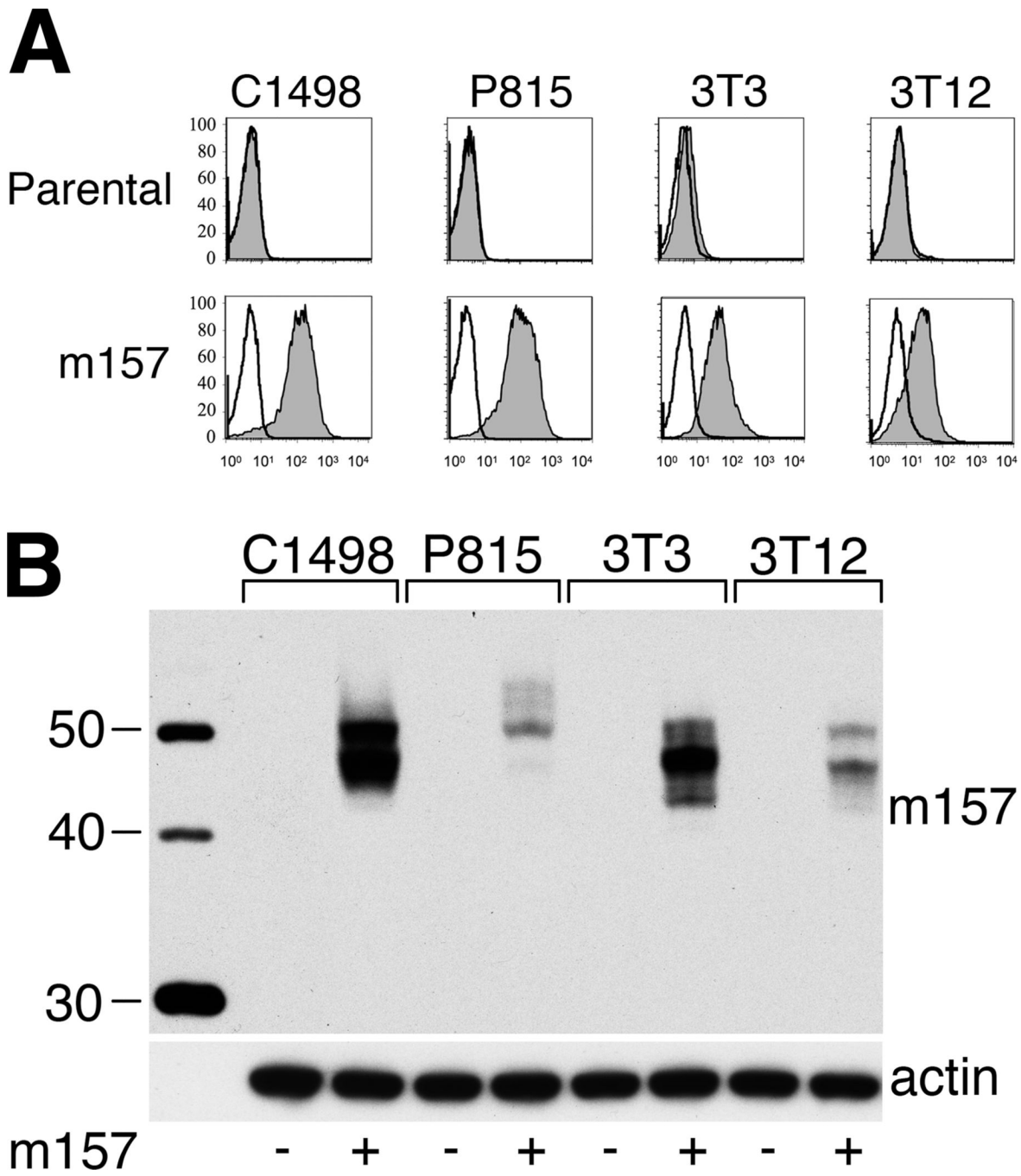

Figure 1. Expression of m157 among different transduced cell types

(A) C1498 (myeloid leukemia), P815 (mastocytoma), NIH-3T3 and 3T12 fibroblast lines (parental and m157-transduced) were evaluated for cell surface expression of m157 by flow cytometry using Cy-5-labeled mAb 6H121 (grey shaded histograms) or isotype control (open histograms). (B) Triton X-100 lysates were prepared from the indicated parental and m157-transduced cell lines and assessed for m157 content by western blotting using mAb 6H121.

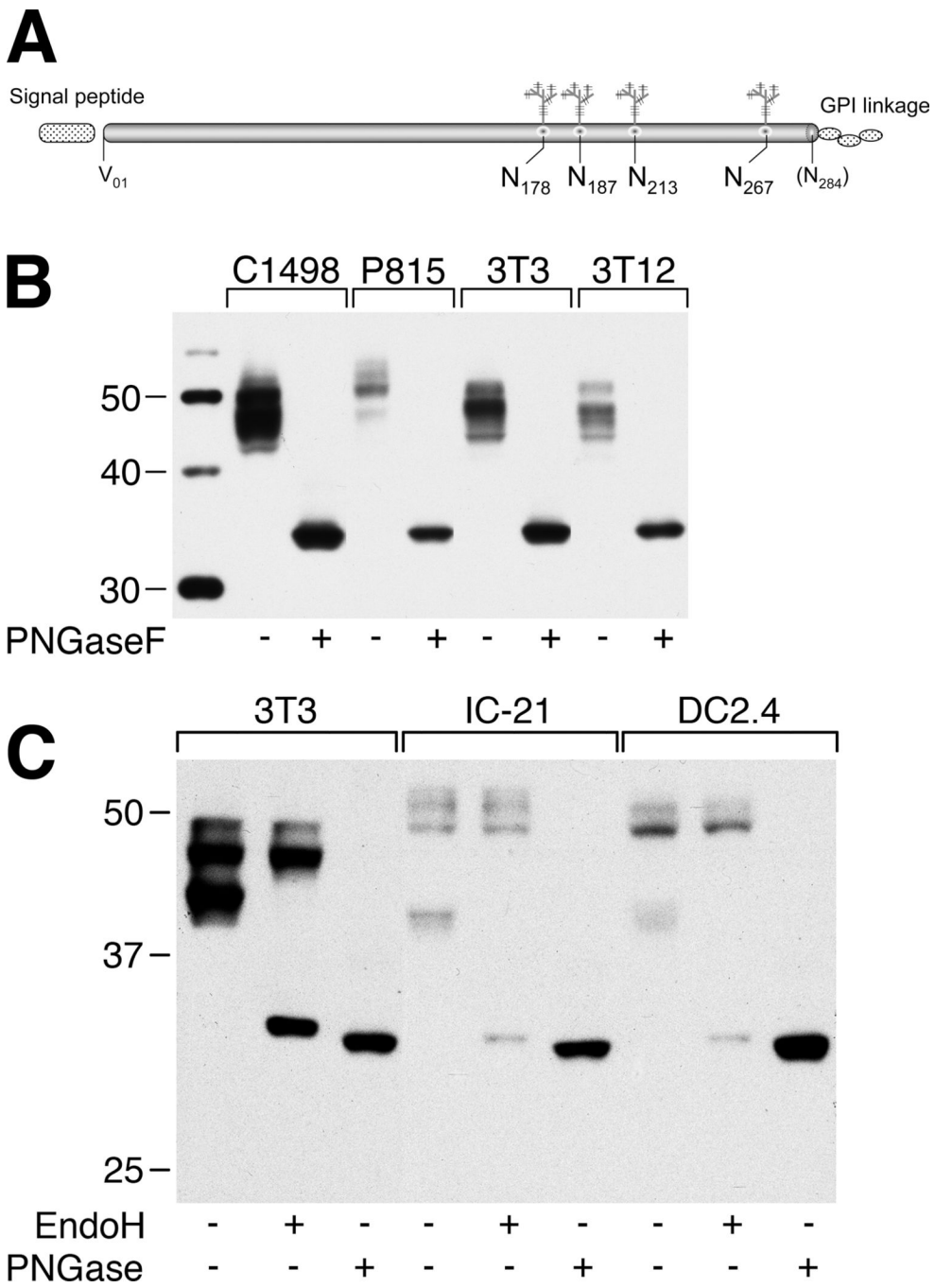

Figure 2. MCMV m157 isoforms result from differential N-linked glycosylation

(A) Schematic depiction of mature m157 protein, residues Ile^{01} through Ser^{286}. The positions of four predicted N-linked glycosylation sites at N178, N187, N213, and N267 are indicated; a fifth site at N284 is not a candidate due to its proximity to the GPI cleavage site at Ser^{286}. (B) Triton X-100 lysates were prepared from the indicated m157-transduced cell lines and aliquots (20 μg proteins) were digested with Endo H or PNGase F to remove N-linked carbohydrates. (C) NIH-3T12 fibroblasts, IC-21 macrophages and DC2.4 dendritic cells were infected with MCMV (K181-derived, GFP-expressing RM4503.3 strain [49]). Triton X-100 lysates from infected cells were subjected to Endo H or PNGase F treatment

followed by western blotting. Note that an ~42 kDa isoform present in all cell lines is Endo H sensitive, but isoforms of higher molecular weight are variable and resistant to Endo H.

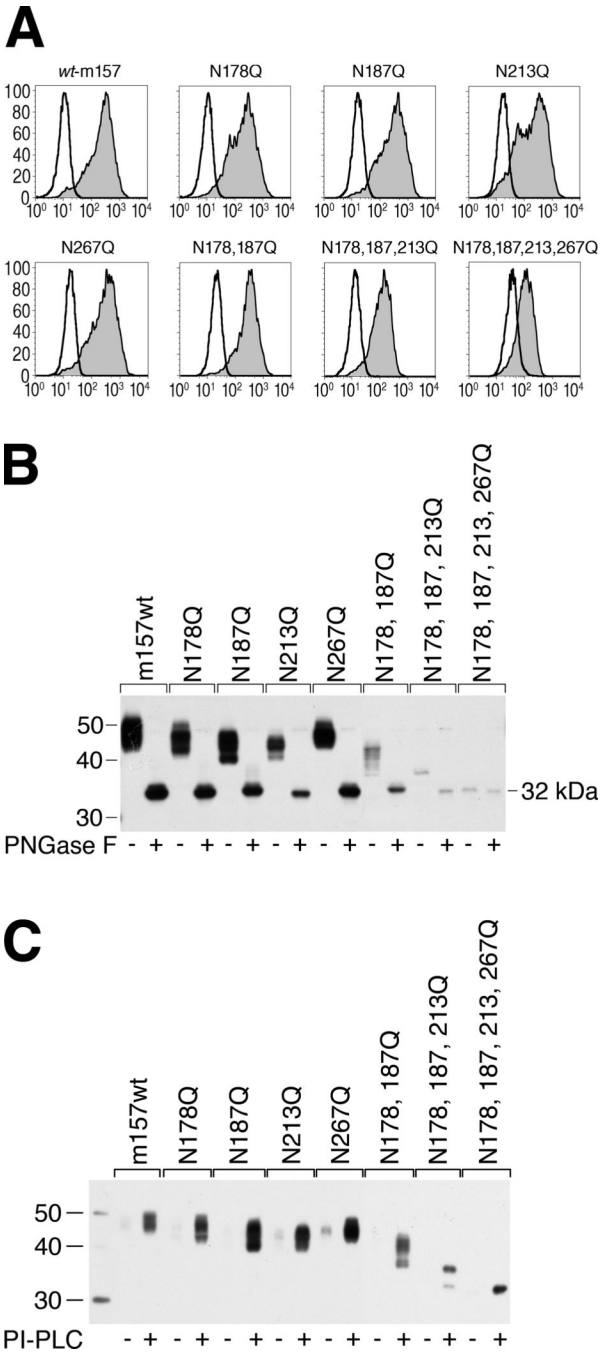

Figure 3. Generation and characterization of single and combinatorial N-glycosylation site mutants of m157 in C1498 cells

(A) Site-directed mutagenesis of asparagine (N)-to-glutamine (Q) was performed to alter each of the four predicted N-glycosylation sites at N178, N187, N213, and N267 in isolation and in double-N178,187Q, triple-N178,187,213Q, and quadruple-N178, 187, 213, 267Q combinations. Each m157 N-glycosylation site mutant was retrovirally expressed in C1498 cells and evaluated for cell surface expression by flow cytometry using mAb 6H121 (shaded histograms) and compared to isotype control (open histograms). (B) Triton X-100 lysates from each of the m157-expressing C1498 lines were subjected to PNGase F treatment and analyzed by western blotting as in Fig. 2. Untreated samples (−) show m157 species of

predictably different sizes, consistent with N-linked glycosylation at the remaining (unmutated) sites, but following PNGase F digestion (+), all m157 species are reduced to ~32 kDa, the predicted size of the unmodified mature polypeptide. (C) C1498 cells lines expressing m157 mutants were treated with PI-PLC or left untreated. 10μl of supernatants were diluted in sample buffer and analyzed by western blotting (thus the relative amount of m157 present in each sample is concentrated compared to the cell lysates depicted in *B*).

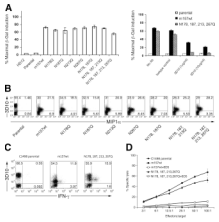

Figure 4. N-glycosylation-deficient m157 retains the capacity to activate Ly49H reporter cells and fresh Ly49H$^+$ NK cells

(A) C1498 cells expressing *wt*-m157 or m157 N-glycosylation site mutants were incubated with Ly49H-expressing HD12 cells and induction of β-galactosidase activity in HD12 cells was measured by CPRG assay and plotted as a percentage of the maximal induction using PMA + ionomycin (all samples assayed in triplicate). Right panel shows not only specificity of the HD12 reporter activity, but also the increased sensitivity of Ly49H-mediated activation by the quadruple-N178,N187,N213,N267 mutant to mAb 3D10 (anti- Ly49H)-mediated blockade. (B) MIP-1α and (C) IFN- γ production by NK cells after incubation with the C1498-m157 panel of cell lines. Freshly isolated B6.RAG1$^{-/-}$ splenocytes were co-cultured for 6 hr with parental C1498, or C1498 cells expressing *wt*-m157 or each of the N-glycosylation site m157 mutants. For each dot plot, cells were gated on the NK1.1$^+$ population. Note that there is comparable intracellular MIP-1α or IFN-γ production in response to all m157-expressing cell lines that correlates with Ly49H receptor downregulation. (D) A representative ^{51}Cr-release assay showing comparable NK cell killing of C1498-m157wt (filled squares) and C1498-m157-N178,187,213,267Q targets (filled triangles), but not parental C1498 cells (filled circles). Preincubation with anti-m157 specific antibodies (6D5, 10 μg/ml, open symbols) specifically blocks killing of m157-expressing targets, but not YAC-1 targets (not shown). Data area representative of 5 (part A) or 3 (part B–D) experiments.

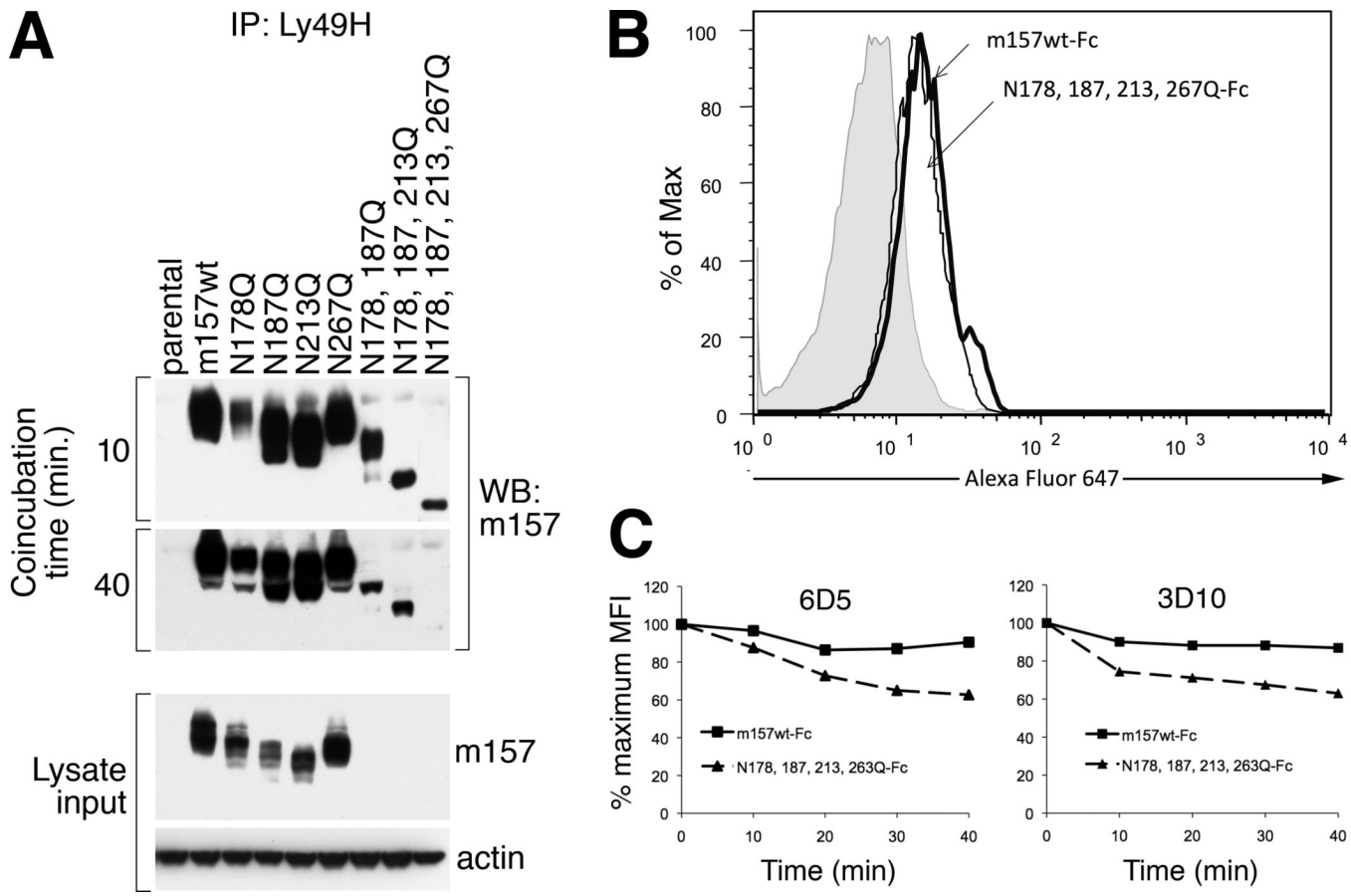

Figure 5. N-glycosylation of m157 enhances the stability of Ly49H-m157 binding

(A) C1498 cells expressing *wt*-m157 or each of the indicated m157 N-glycosylation site mutants were incubated with Ly49H-expressing HD12 cells for 10–40 min. at 37°C. Cell mixtures were lysed in IP buffer and Ly49H was immunoprecipitated with mAb 3D10. 3D10 precipitates following 10 or 40 min coincubation (top panels) and whole cell lysates (bottom panel) were then analyzed by western blotting using mAb 6H121 to detect coimmunoprecipitated m157 as in Figs. 2 and 3. Note that the blots are intentionally overexposed to clearly show interactions between Ly49H and the combinatorial N-glycosylation mutants, which are expressed at an apparent lower abundance. The m157-Ly49H interactions are uniformly stable with the exception of the quadruple-N178,187,213,267Q mutant, which loses its interaction with Ly49H after 40 min of coincubation. (B) HD12 cells were incubated with Alexa-fluor 647-labeled soluble m157wt-Fc or N178,187,213,267Q-Fc reagents for 15 min at room temperature, washed and analysis by flow cytometry. Note MFI of HD12 stained with m157wt-Fc and N178,187,213,267Q-Fc are nearly identical. (C) Kinetic dissociation of Alexa Fluor-647-labeled m157-Fc from HD12 cells. Ly49H-expressing HD12 cells were incubated with labeled m157wt-Fc or N178,187,213,267Q-Fc as in (B); at time 0, blocking mAbs 6D5 or 3D10 (unlabeled) were added at room temperature and individual samples were analyzed sequentially by flow cytometry after 10, 20, 30 and 40 min incubation. Data are expressed as the percentage of the maximum MFI (time 0 = 100%; see part B). Data are representative of 4 experiments.

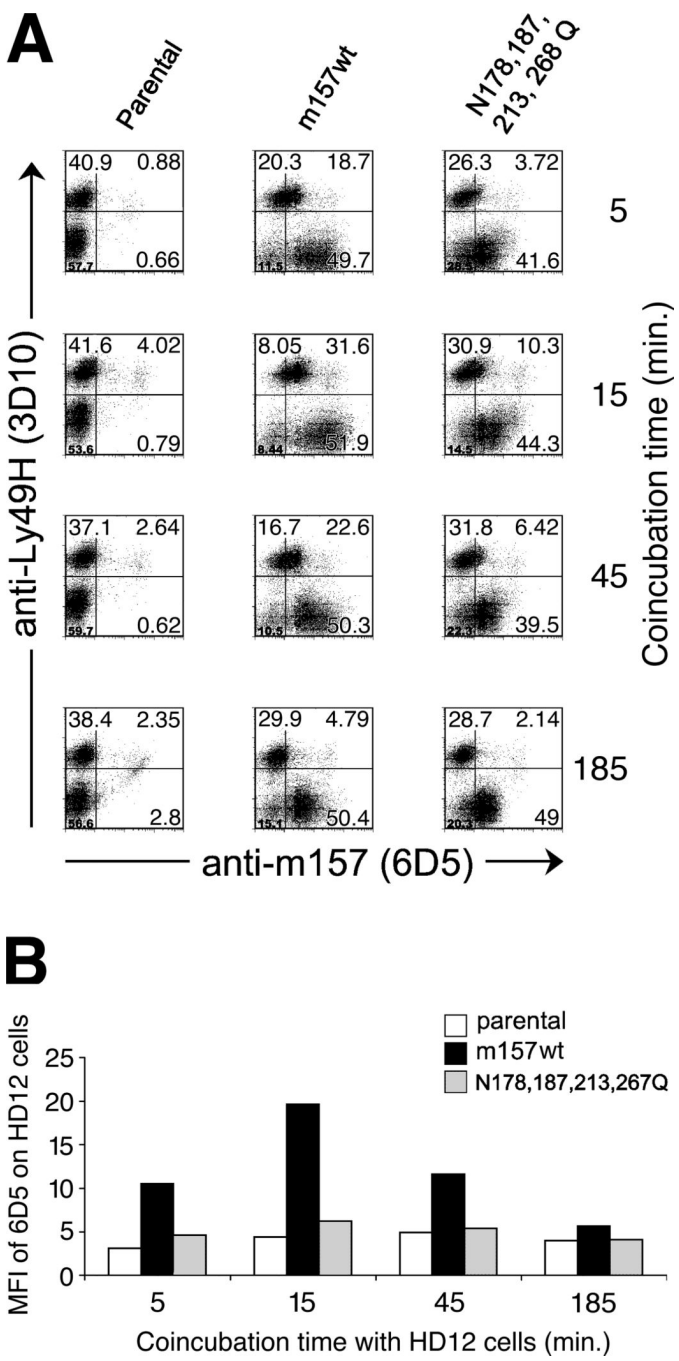

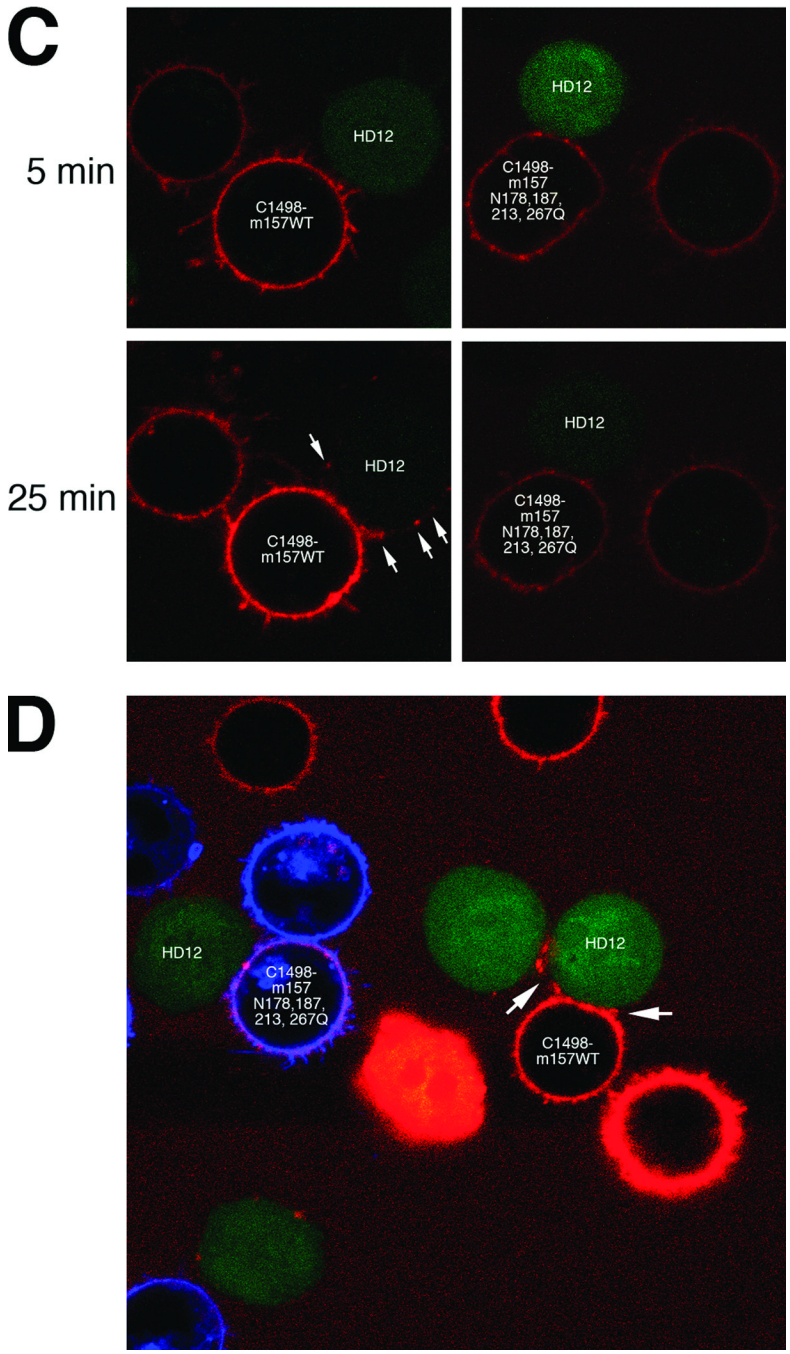

Figure 6. N-glycosylation of m157 enhances trogocytosis by Ly49H-expressing cells

(A) Flow cytometric analysis of Ly49H-expressing HD12 cells mixed (1:1) with parental C1498 cells (left column), C1498-m157wt cells (middle column), or C1498-m157-N178,187,213,267N cells expressing unglycosylated m157 (right column) at the indicated times of coincubation. Cell mixtures were stained for surface expression of Ly49H (3D10-PE) and m157 (6D5-APC); HD12 cells were prelabeled with CFSE (not shown) to facilitate discrimination within the cell mixtures. Only single cell events were collected by means of scatter gating. (B) Graphical depiction of density of m157 (MFI of APC-6D5) on Ly49H-expressing HD12 cells in each cell mixture at the indicated times of coincubation. The lack of N-glycosylation on m157 dramatically reduces this parameter of the receptor-ligand

interaction at all time points up to 3 hr. (C) Representative live cell images of C1498-m157wt (left panel) or C1498-m157-N178,187,213,267N mutant (right panel) coincubated with HD12 cells (labeled with CFSE). Cells were mixed (1:1) on glass bottom culture dish and incubated for 5 min at 37 °C. Addition of Cy5-6D5 stained m157-expressing cells in red. Images were taken every 2 min; the images at 5 and 25 min are shown. Arrows indicate points at the surface of HD12 cells (red spots) where transfer of w*t*-m157 has occurred (left panel). No transfer of unglycosylated m157 to HD12 cells was observed (right panel). (D) CFSE-labeled HD12 cells (green) were mixed with PKH-26-labeled C1498-m157-N178,187,213,267N mutant cells (blue) together with unlabeled C1498-m157wt cells (1:1:1) and incubated for 15 min at 37 °C. Addition of Cy5-6D5 (anti-m157) to cell mixture stains C1498-m157wt cells red, whereas C1498-m157-N178,187,213,267N mutant cells appear pink. Images were taken every 2 min for 10 min; the final image is shown. Arrows indicate a transfer of *wt*-m157 from C1498-m157wt (red) to HD12 (green) cells that was not observed for HD12 cells contacting C1498 cells expressing unglycosylated m157. Data are representative of 3 (parts A, B) and 5 (parts C, D) experiments, respectively.